18TH WORLD CONFERENCE ON EARTHQUAKE ENGINEERING
WCEE2024
MILAN

MILAN, ITALY
30TH JUNE - 5TH JULY 2024
www.wcee2024.it

PARAMETRIC ANALYSIS ON THE SEISMIC RESPONSE OF SELF-CENTERING DISSIPATIVE SDOF SYSTEMS

L. Pieroni[1*], F. Freddi[1], M. Latour[2], E. Tubaldi[3]

[1] Department of Civil, Environmental and Geomatic Engineering, University College London, UK, *ludovica.pieroni.20@ucl.ac.uk

[2] Department of Civil Engineering, University of Salerno, Fisciano, Italy

[3] Department of Civil and Environmental Engineering, University of Strathclyde, Glasgow, UK

Abstract: *Innovative solutions in Earthquake Engineering are pushing the boundaries towards the design of seismic-resilient structures able not only to meet the life safety requirements, but also to overcome rare earthquakes with limited damage, thus reducing repair costs and downtime. Self-Centering Dissipative (SCD) systems represent an efficient solution to meet this goal, thanks to their capacity to reduce structural damage and avoid residual drifts. Although the performance benefits have been widely demonstrated, their application in practice is still limited due to the lack of general methodologies and code provisions regarding their design and use. Featuring a distinctive flag-shaped hysteresis behaviour, SCD systems exhibit reduced energy dissipation capabilities compared to conventional non-linear systems. This may lead to high displacement and acceleration demands, making conventional design assumptions inapplicable and unsafe. Within this context, determining the relationship between the inelastic demand of SCD systems and equivalent linear systems with the same initial stiffness and damping ratio is a key aspect of the definition of simplified design procedures. The present study performs a parametric analysis on SCD Single Degree of Freedom (SDoF) systems with various hysteretic properties as defined by the initial stiffness, post-yielding hardening, energy dissipation capacity, and displacement ductility. For each configuration, non-linear time-history analyses are performed in Opensees with a set of 240 ground motions scaled to reach a target ductility value, while evaluating the influence of the hysteretic properties on the statistics of the demands. Moreover, constant-ductility spectra are defined in terms of displacements and accelerations. The results inform methods for predicting the seismic demands for SCD systems based on the equivalent elastic system, which is useful information for the definition of simplified design procedures.*

1 Introduction

Earthquakes are among the deadliest and costliest catastrophic events worldwide, posing significant threats to people and the built environment. The earthquake engineering community is now focused on developing lateral force-resisting systems that fulfil both life-safety and functional recovery requirements. The primary goal is to prevent casualties and ensure that a structure can be quickly and economically restored after an earthquake (*e.g.,* EERI 2019, Freddi *et al*. 2021). In this context, Self-Centering Dissipative (SCD) systems have emerged as a promising solution, ensuring life safety and minimal damage while keeping residual drifts negligible (Zhong & Christopoulos 2022, Fang *et al*. 2022). These systems dissipate seismic energy in specific components, such as friction dampers or yielding elements, acting as fuses. They also provide self-centring behaviour through specific elements, such as post-tensioned steel rods or special materials, which restore the structure to its original position after an earthquake.

Many analytical, experimental, and numerical studies have confirmed the effectiveness of SCD systems in enhancing the seismic performance of structures (Karavasilis *et al.* 2011, Dimopoulos *et al.* 2013, Pei *et al.* 2019, Latour *et al.* 2019, Freddi *et al.* 2020, Wang *et al.* 2021, Shen *et al.* 2022). Despite these advances, the

practical application of SCD systems remains limited, as no established methodologies and code provisions exist for their design and implementation (Pieroni *et al.* 2022). In this context, academic efforts are needed to generalize prior academic findings and foster the knowledge transfer from academia to building codes, advancing the use of SCD systems in construction practice.

This research endeavour was initiated by Christopoulos *et al.* (Christopoulos *et al.* 2002, Seo & Sauce 2005), who conducted parametric studies on the inelastic demand of SCD SDoF systems when subjected to acceleration time histories. Both studies considered a set of earthquake records and investigated several hysteretic behaviours (*i.e.,* flag-shape and bilinear plastic) with different initial and post-yielding stiffness and yielding strength. Predictably, the results showed that due to their flag-shape hysteretic behaviour, SCD systems dissipate less energy than conventional Bilinear Plastic (BP) systems, leading to higher displacement and acceleration demands. These findings were confirmed for SCD multi-degree of freedom systems by Pieroni *et al.* and Lettieri *et al.* (Pieroni *et al.* 2022, Lettieri *et al.* 2023).

These findings shed light on the comparison between the behaviour of SCD and BP SDoF systems; nevertheless, the development of a reliable and consistent design procedure remains a crucial aspect to be addressed. For this purpose, determining the relationship between the inelastic demand of non-linear SDoF systems and the equivalent Linear Elastic (LE) systems with the same initial stiffness and damping ratio is a key aspect for the definition of simplified design procedures. While estimates were developed for bilinear plastic SDoF systems (see *e.g.*, Veletsos & Newmark 1960, Miranda 2000), there is limited information on how to relate the demand of SCD SDoF systems to elastic demands.

A recent study extended the Displacement-Based Design approach via Inelastic Displacement Ratio (C_μ) to SCD systems (Priestley *et al.* 2007, De Francesco 2019). A statistical and analytical characterization of C_μ (*i.e.*, the ratio between the peak displacement of the non-linear SDoF system and the equivalent elastic SDoF system) was developed for SCD systems to estimate their inelastic demands based on the elastic demand. Analytical formulations for the estimates of C_μ were provided for SCD systems based on ductility, initial and post-yielding stiffness, and energy dissipation capacity. This was a pivoting study in the definition of a consistent and simplified design procedure for SCD systems; nevertheless, only two scenarios of energy dissipation capacity were investigated, and inelastic demands, such as forces, accelerations, and residual drifts, were not assessed.

The present study aims to relate the inelastic demand of SCD SDoF systems to the demand of equivalent elastic SDoF systems subjected to the same acceleration time histories. A parametric analysis is developed by investigating a large number of SDoF systems with different properties of the hysteretic behaviour, such as initial stiffness, post-yielding hardening, energy dissipation capacity, and ductility. For each SDoF system, non-linear time-history analyses are performed in Opensees with a set of 240 ground motions scaled to reach a target displacement ductility. Constant-ductility spectra are defined for displacements and accelerations as the ratio between the maximum inelastic demand of the SCD SDoF system and the maximum demand of the equivalent elastic SDoF system. The results inform the development of simplified methods for predicting the inelastic demands for SCD SDoF to be used in the design.

2 Self-Centering Dissipative System

Figure 1 (a) shows the force-displacement behaviour of three different SDoF systems when subjected to the same acceleration time history. These systems comprise *i)* a non-linear SCD-SDoF system, *ii)* the equivalent LE SDoF system with the same initial elastic stiffness (k_0) and viscous damping factor (ξ), *iii)* the equivalent BP SDoF system with the same elastic and post yielding stiffness (k_0, k_1) and viscous damping factor (ξ).

As demonstrated in the literature (Veletsos & Newmark 1960), BP SDoF systems with long fundamental periods of vibration have inelastic displacement demands that can be assumed to be conservatively equal to the elastic demand of the equivalent LE SDoF system (*i.e.,* equal displacement rule). The estimation of the inelastic displacement of BP systems from elastic demands was extensively studied, and several simplified yet reliable analytical formulations were provided considering the influence of ground motions' characteristics (*i.e.,* soil conditions, earthquake magnitude, and epicentral distance) and hysteretic properties (*i.e.,* hysteretic shape, post-yielding stiffness ratio, unloading stiffness) (Miranda 2000). Nevertheless, these estimates are not valid for SCD SDoF systems. Being characterized by a flag-shape force-displacement behaviour, these

systems dissipate less energy than the equivalent EP SDoF system (*i.e.,* a smaller area enclosed by the force-displacement curve), leading to higher inelastic displacement demands.

Figure 1 (b) shows the main characteristics of a SCD SDoF system compared to its equivalent LE system. In this Figure, k_0 is the initial stiffness, F_y and u_y are, respectively, the force and displacement at yielding of the SCD SDoF system, and k_1 is the post-yielding stiffness. When subjected to an acceleration time history, u_m, F_m, and a_m are the peak displacement, force, and acceleration of the SCD system, while u_0, F_0, and a_0 are the equivalent parameters for the LE SDoF system. F_d is the forward-to-reverse activation force and is a measure of the energy dissipated by the SCD SDoF system.

The behaviour of the SCD SDoF system is entirely defined by four properties: the initial stiffness (k_0), the post-yielding stiffness ratio (α), the displacement ductility ratio (μ), and the energy dissipation coefficient (β) that can be calculated as follows.

$$\alpha = \frac{k_1}{k_0} \quad , \quad \beta = \frac{F_d}{F_y} \quad , \quad \mu = \frac{u_{max}}{u_y} \tag{1}$$

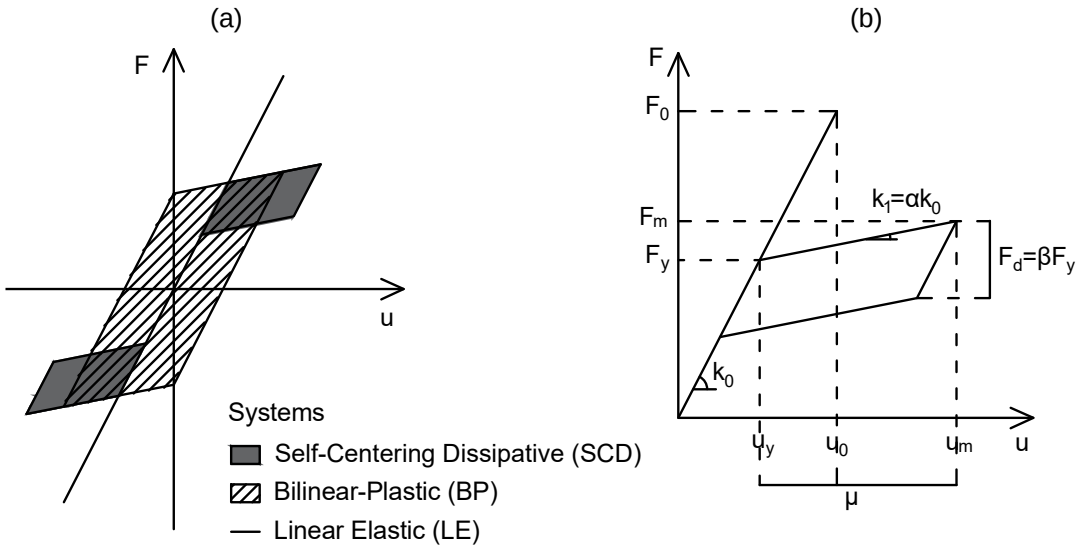

Figure 1:(a) Force-Displacement behaviour of Self Centering Dissipative SDoF systems and equivalent Linear Elastic and Bilinear Plastic systems. (b) Main hysteretic properties of the flag-shape behaviour.

3 Parametric Study

The present study aims to relate the inelastic demand of SCD SDoF systems to the elastic demand of equivalent LE SDoF systems subjected to the same acceleration time histories. To this purpose, the present study performs an extensive parametric analysis by investigating a large number of SDoF systems with different properties of hysteretic behaviour, following a non-dimensional approach employed by some of the authors of this study to analyse other type of systems (Tubaldi *et al.*, 2014). Specifically, 108 SDoF systems are defined, combining different values of T, β, α, and μ that are chosen as follows:

- Four values of T are selected (*i.e.*, 0.3, 0.9, 1.5, 2.0 s).
- Three values of β are considered to investigate the effect of the energy dissipation capacity (*i.e.*, 0, 0.4, 1). It is worth specifying that β=0 is related to systems with no energy dissipation (*i.e.*, no hysteresis loop, bilinear hyper elastic systems), β=1 is associated with SCD systems with the maximum dissipated energy while ensuring a full self-centering capability.
- Three values of α are taken into account according to admissible values of post-yielding hardening for self-centering systems (*i.e.*, 0%, 5%, 20%) (Seo & Sauce 2005). α=0% is associated with elastoplastic systems.
- Three values of μ are considered to cover a wide range of potential scenarios (*i.e.*, 1, 4, 8). μ=1 is indicative of elastic systems.

For all SDoF systems, the damping ratio is assumed to be ξ=0.03, which is a reference value typically used for steel structures. k_0 is defined based on T and m (*i.e.*, $k_0 = m\omega^2 = m(2\pi/T)^2$ where ω is the circular frequency).

For each SDoF system, non-linear time history analyses are performed in Opensees using a set of 240 ground motion records to account for the influence of the uncertainty related to the earthquake input (*i.e.*, the record-to-record variability). Figure 2 (a) shows the spectra in pseudo acceleration ($S_A(T, \xi)$) of the selected ground motions. The considered set was selected by Baker *et al.* (Baker *et al.* 2011) for the analysis of a variety of structural systems located in active seismic regions. A large number of zeros acceleration points (*i.e.*, 40 s) were added at the end of each record to allow the free vibrations to stop and to correctly capture the residual displacements.

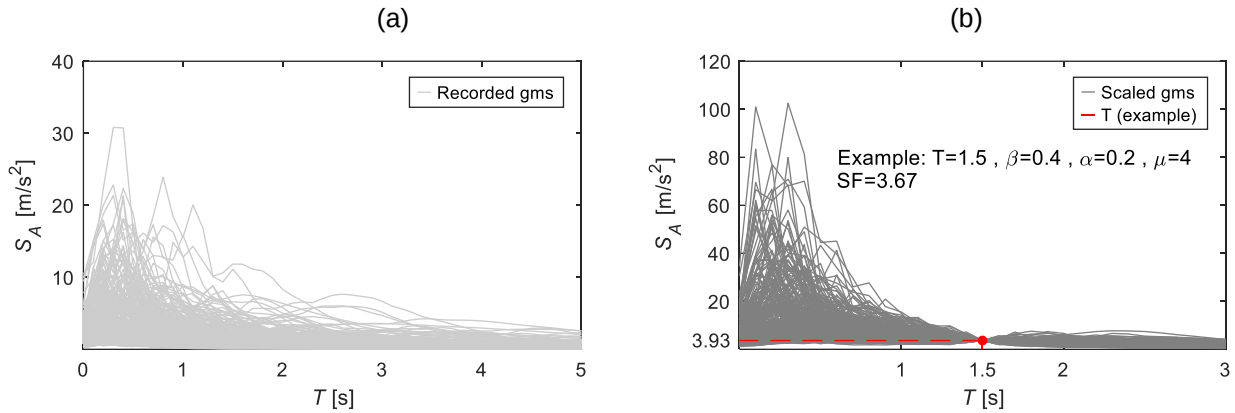

Figure 2:(a) Unscaled ground motions (gms). (b) Example of scaled ground motions for a SCD SDoF system to reach the target ductility.

Figure 3 shows a schematic representation of the model developed in Opensees (McKenna *et al.* 2010) for the SDoF systems. It consists of a truss element fixed at one end (*i.e.*, node 1) and connected to a mass at the other end (*i.e.*, node 2) that has roller support. The truss is assigned length L=1 m and cross-sectional area A=1m^2. The mass is applied in node 2 and assumed to be equal to m=1 kg. The non-linear response of the element is modelled by 'uniaxial Self Centering' material in the cases of β equal to 0, 0.4, and 0.8 and 'uniaxial Steel01' material in the case of β equal to 2. An arbitrary value is assigned to the yielding force, F_y = 1N. During the non-linear time history analyses, the displacement and acceleration of node 2 are recorded, together with the axial force in the truss.

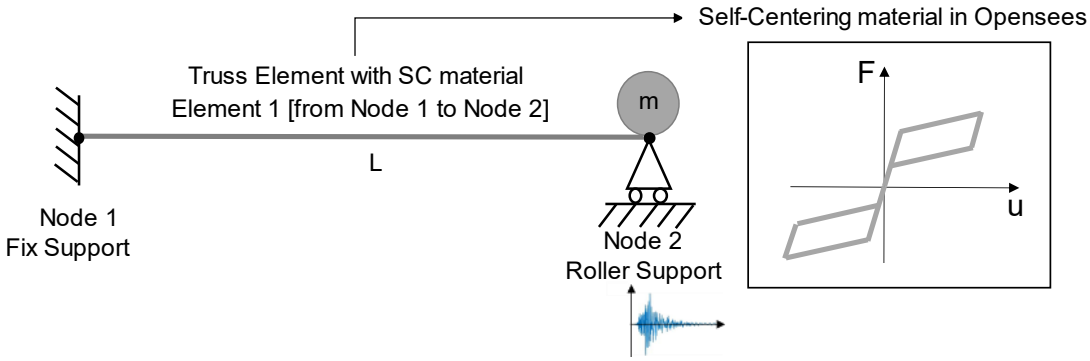

Figure 3: Schematic of the model developed in Opensees.

For each SDoF system, the 240 ground motions are scaled to have a pseudo-spectral acceleration $S_A(T, \xi)$=1m/s^2. Subsequently, a Scale Factor (SF) is applied to these ground motions such that the mean value of peak displacement ductility ($\bar{\mu}$) is within a 0.1% tolerance of the target ductility (μ). All the ground motion have the same values of pseudo-spectral acceleration equal to $S_A(T, \xi)=SF$ m/s^2. The iterative scaling process to reach the target ductility requires significant computational effort and time (Freddi *et al.* 2021). Once the target ductility is reached ($\bar{\mu}\sim\mu$) and the associated scaling factor is defined (SF_μ), the demands of the considered SDoF system and the equivalent LE SDoF system that need to withstand the same input without yielding can be defined. Figure 2 (b) shows the linear elastic spectra in pseudo acceleration $S_A(T, \xi)$ of the selected ground

motions for the SCD SDoF system with T=1.5 s, β=0.4, α=0.2. The scaling factor obtained to reach the target ductility μ=4 is SF_μ=3.67 and all ground motions are scaled to the same value of $S_A(1.5, \xi)$= SF_μ.

The values of u_0, F_0, and a_0 of the equivalent LE SDoF system under the 240 motion records can be calculated as follows:

$$a_0 = \mathrm{SF}_\mu \quad ; \quad F_0 = m \cdot a_0 = m \cdot \mathrm{SF}_\mu \quad ; \quad u_o = \frac{F_o}{k_0} \tag{2}$$

To relate the investigated SDoF systems to the equivalent LE SDoF system, constant-ductility spectra are defined in terms of displacement and accelerations as follows.

- Constant ductility inelastic displacement ratio (C_μ)

$$C_\mu = \frac{\overline{u_m}}{u_o} \tag{3}$$

where $\overline{u_m}$ is the mean peak displacement among the 240 motion records.
C_μ is a measure of the difference between the seismic behaviour of elastic and inelastic systems in terms of maximum displacement. If information on C_μ is available, the maximum inelastic displacement of SCD SDoF system can be estimated based on the response of the equivalent LE SDoF system in terms of u_0. For BP SDoF systems with long fundamental periods of vibration, $C_\mu \approx 1$ according to the equal displacement rule (Veletsos & Newmark 1960).

- Constant ductility inelastic acceleration ratio (A_μ):

$$A_\mu = \frac{\bar{a}_m}{a_0} = \frac{\bar{a}_m}{\mathrm{SF}_\mu} \tag{4}$$

where $\overline{a_m}$ is the mean peak acceleration among the 240 motion records.
A_μ is a measure of the relative performance of the SCD system compared to the EL system in terms of accelerations.

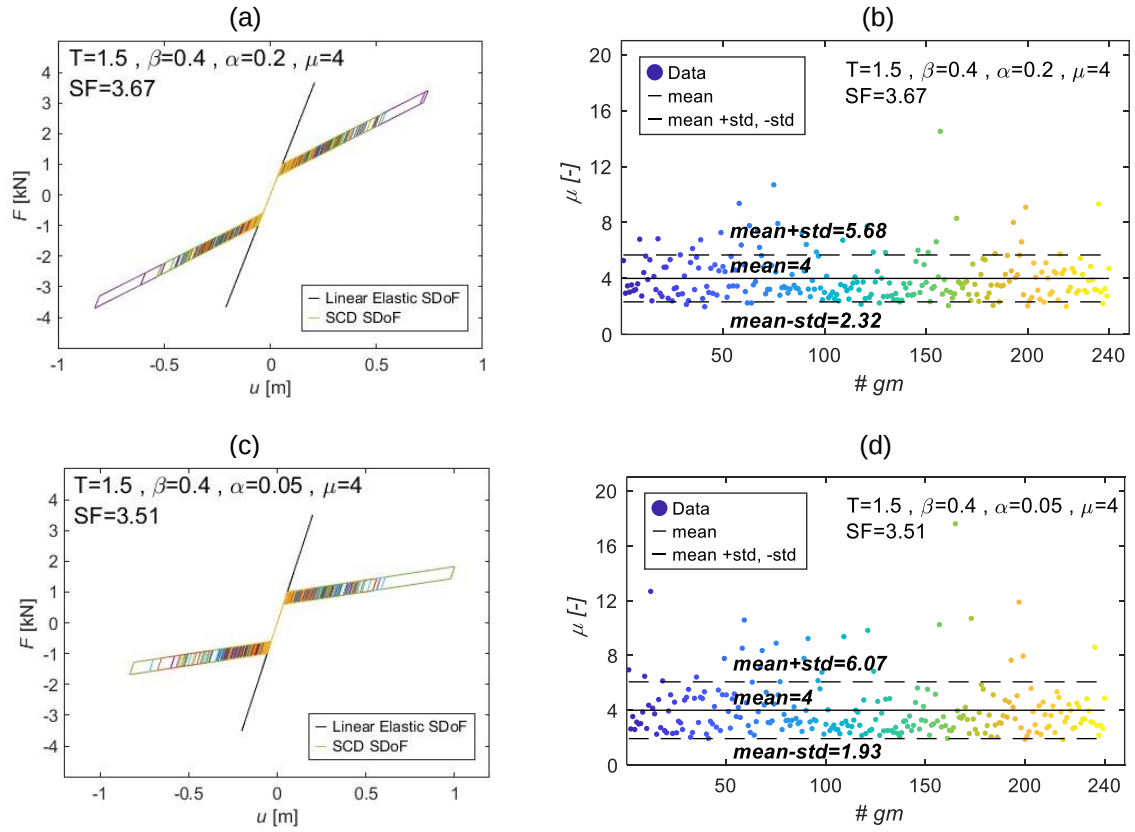

Figure 4: Results of the scaling process for two SCD SDoF systems with (T, β, α, and μ). (a), (c) Force-displacement behaviour. (b), (d) Values of ductility.

Figure 4 (a) and (b) show the flag shape behaviour and the displacement ductility obtained from the 240 ground motion records after the scaling process for the SCD SDoF system with T=1.5 s, β=0.4, α=0.2, and μ=4. The scaling factor obtained to reach the target ductility μ=4 is SF_μ=3.67. Figure 4 (a) shows the force-displacement flag shape behaviour of the SCD SDoF system obtained from the 240-scaled ground motion and the equivalent LE SDoF system that has F_0=3.67 m/s^2. In Figure 4 (b) the dots represent the values of μ for the SCD SDoF system obtained from the 240-scaled ground motion, while the black line is the mean value of μ among all the ground motions and is $\bar{\mu}\approx$4. Figure 4 (c) and (d) show the results for another SCD SDoF system with T=1.5 s, β=0.4, α=0.05, and μ=4 and the obtained scaling factor is SF_μ=3.51.

Figure 5 shows the results of C_μ and A_μ for the two SCD SDoF systems considered in Figure 4. For each period the grey dots represent the values obtained from the 240 ground motion records scaled at $S_A(T, \xi)= SF_\mu$ to reach the target ductility. The black line represents the mean values, and the dotted lines represent the mean plus and minus the standard deviation showing the variability of the results.

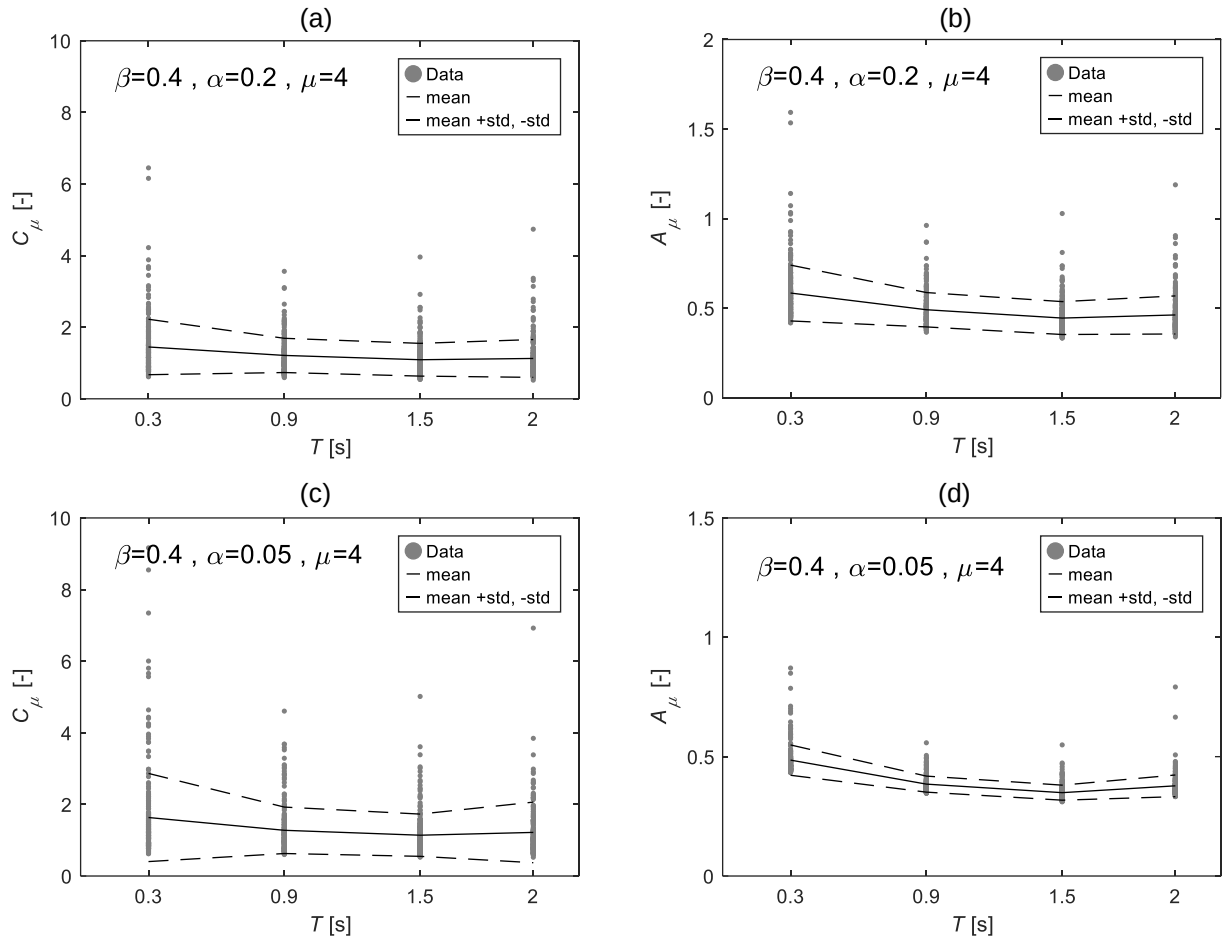

Figure 5:(a) Constant ductility inelastic displacement ratio. (b) Constant ductility acceleration ratio for two SCD SDoF systems with (β, α, and μ) and different values of period (T).

4 Constant ductility spectra

Figure 6 illustrates the constant ductility spectra obtained for few combinations of the parameters describing the SDoF system's properties (T, β, α, and μ). It is worth mentioning that the spectra are based on mean values of the quantities among the 240 ground motion records.

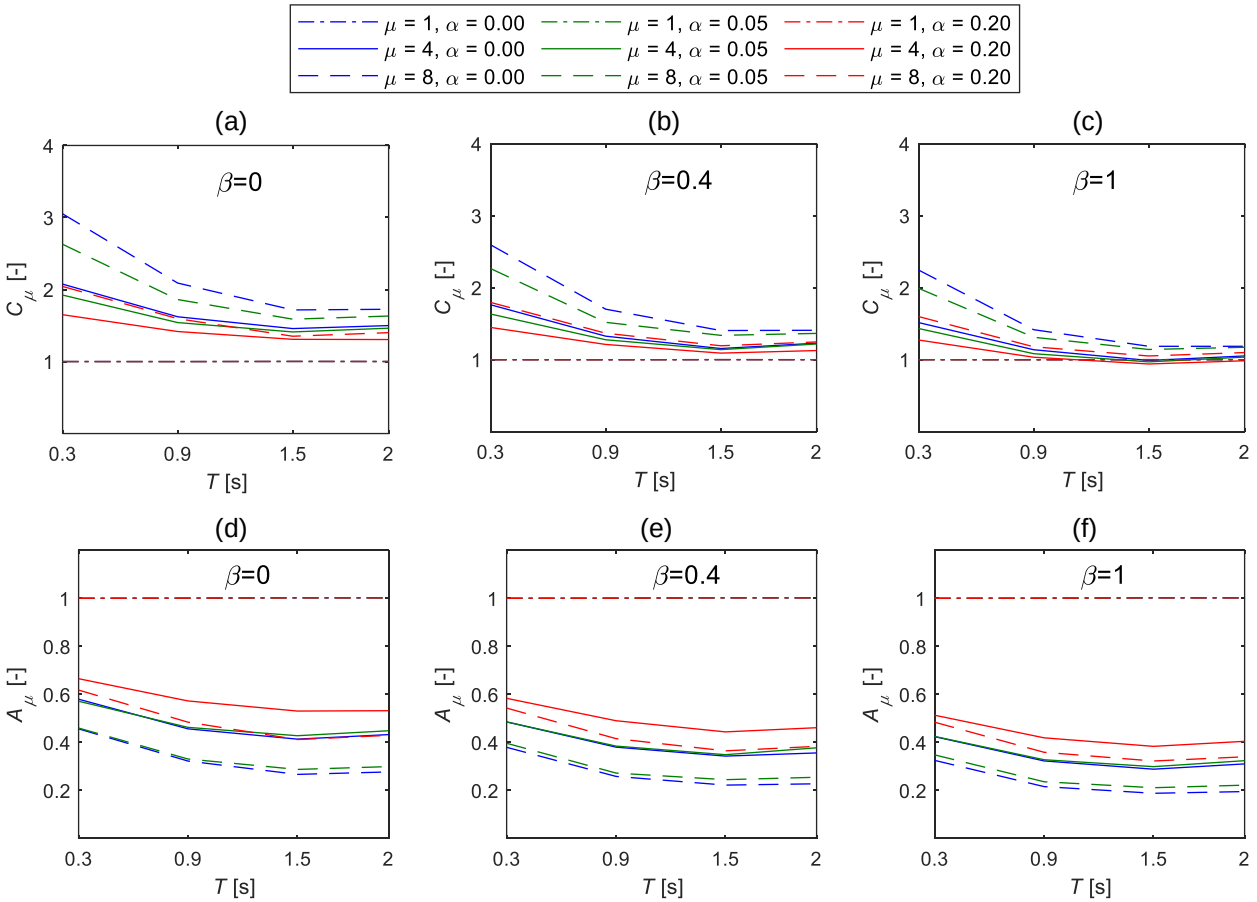

Figure 6: Constant ductility spectra for SDoF systems with different hysteretic properties. (a)-(c) Constant ductility inelastic displacement ratio. (d)-(f) Constant ductility acceleration ratio.

Figure 6 (a-c) show the obtained spectra for inelastic displacement ratio (C_μ). The lower bound for C_μ is 1, representing a SCD SDoF system experiencing the same peak displacement than the equivalent LE SDoF system. It is observed that given a value of β, C_μ increases for increasing values of μ and decreasing values of α. For example, C_μ associated with μ=8 (dotted lines) is larger than C_μ associated with μ=4 (continuous lines) for all the values of T and α. On the other hand, C_μ associated with α=0 (blue lines) is larger than C_μ associated with α=0.2 (red lines) for all the values of T and μ. This means that SCD SDoF systems with larger displacement ductility (μ) and smaller post-yielding ratios (α) experience larger peak displacements. Increasing the value of β, C_μ decreases. This means that increasing the energy dissipation leads to smaller peak displacements, and the response of SCD SDoF systems is similar to the equivalent BL SDoF systems. For long periods and increasing values of β, C_μ tends to 1, according to the equal displacement rule. Nevertheless, it's important to mention that in some cases, C_μ is below 1, indicating that that the inelastic displacement demand is smaller the elastic displacement demand. This finding aligns with results from prior studies (De Francesco 2019).

Figure 6 (d-f) show the constant ductility inelastic acceleration ratio spectra (A_μ). The upper bound for values of A_μ is 1 as the investigated SDoF systems experience the same peak acceleration or smaller than the equivalent LE SDoF system. It is observed that given a value of β, A_μ increases for decreased values of μ and increased values of α. For example, A_μ associated with μ=4 (dotted lines) is larger than A_μ associated with μ=8 (continuous lines) for all the values of T and α. Whereas, A_μ associated with α=0.2 (blue lines) is larger than A_μ associated with α=0.2 (red lines) for all the values of T and μ. This means that SCD SDoF systems with smaller displacement ductility (μ) and larger post-yielding ratios (α) experience larger peak accelerations. Increasing the value of β, A_μ decreases, although A_μ is less sensitive to β than C_μ. This means that increasing the energy dissipation leads to smaller peak accelerations.

It is worth mentioning that the cases with μ=1 represent LE SDoF systems; therefore C_μ=1 and A_μ=1 for all values of T, β and α.

5 Conclusions

The present study aims to investigate the relationship between the inelastic demand of Self-Centering Dissipative (SCD) Single Degree of Freedom (SDoF) systems and the demand of equivalent elastic SDoF systems with the same initial stiffness and damping ratio when subjected to earthquake excitation. A parametric analysis is carried out by investigating a large number of SDoF systems with different properties of the hysteretic behaviour, such as initial stiffness, post-yielding hardening, energy dissipation capacity, and ductility. For each SDoF system, non-linear time-history analyses are performed in Opensees with a set of 240 ground motions scaled to reach a target displacement ductility. Constant-ductility spectra are defined for the inelastic displacement ratio (C_μ) and acceleration ratio (A_μ), defined as the ratio between the maximum inelastic demand of the SCD SDoF system and the maximum demand of the equivalent elastic SDoF system.

The results show that SCD SDoF systems experience larger peak displacements than the equivalent linear elastic SDoF system. Increasing the energy dissipation capacity and the post-yielding ratio and decreasing the displacement ductility leads to smaller peak displacements of the SCD SDoF system. For long periods and increased vales of energy dissipation capacity, the peak displacements of the SCD SDoF system tend to the elastic displacement of the equivalent linear elastic SDoF system. Peak accelerations are less sensitive to the energy dissipation capacity and increase, decreasing the displacement ductility and increasing the post-yielding ratio. The results inform simplified methods for predicting the inelastic demands for SCD SDoF to be used in simplified design procedures.

Future developments will include the extension of the parametric study to more values of initial stiffness, post-yielding hardening, energy dissipation capacity, and ductility. Specifically, cases with energy dissipation capacity (β) between 1 and 2 will be investigated to consider SCD SDoF systems without a fully self-centering behaviour. Constant ductility spectra in terms of strength reduction factor (R_μ, *i.e.*, the ratio between the peak force of the equivalent linear elastic SDoF system and the yielding force of the SCD SDoF system) will be added. Statistical and analytical characterization of C_μ, A_μ, and R_μ will be developed to predict the demands of SCD SDoF systems by starting from equivalent EL systems, without performing non-linear time history analyses.

6 Acknowledgements

The Authors also acknowledge the support from the Royal Society - International Exchange programme under the grant agreement IES\R3\213175. Any opinions, findings, conclusions and/or recommendations expressed in this paper are those of the authors and do not necessarily reflect the views of the Funders.

7 References

Baker J.W., Jayaram N., Shahi S. (2011/03). New ground motion selection procedures and selected motions for the PEER transportation research program. PEER Technical Report, Berkeley, CA.

Christopoulos C, Filiatrault A, Folz B. (2002). Seismic response of self-centering hysteretic SDOF systems. *Earthquake Engineering And Structural Dynamic*. 31:1131-1150.

De Francesco G. (2019) Constant-ductility inelastic displacement ratios for displacement-based seismic design of self-centering structures. *Earthquake Engineering Structural Dynamic.* 48:188–209

Dimopoulos, A.I., Karavasilis, T.L., Vasdravellis, G. Brian Uy. (2013). Seismic design, modelling and assessment of self-centering steel frames using post-tensioned connections with web hourglass shape pins. *Bulletin of Earthquake Engineering* 11: 1797–1816.

Earthquake Engineering Research Institute. Functional Recovery: A Conceptual Framework with Policy Options. (2019).

Fang C., Wang W., Qiu C., Hu S., Macrae G.A., Eatherton M.R. (2022). Seismic resilient steel structures: A review of research, practice, challenges and opportunities. *Journal of Constructional Steel Research*. 191: 107172

Freddi F., Dimopoulos C.A., Karavasilis T.L. (2020). Experimental evaluation of a rocking damage-free steel column base with friction devices, *ASCE Journal of Structural Engineering*. 146(10): 04020217.

Freddi F., Galasso C., Cremen G., Dall'Asta A., Di Sarno L., Giaralis A., Guti´errez-Urzúa F., Malaga Chuquitaype C., Mitoulis S.A., Petrone C., Sextos A., Sousa L., Tarbali K., Tubaldi E., Wardman J., Woo

G. (2021). Innovations in earthquake risk reduction for resilience: recent advances and challenges. *International Journal of Disaster Risk Reduction*. 60:102267.

Freddi, F, Tubaldi, E, Zona, A, Dall' Asta, A. Seismic performance of dual systems coupling moment-resisting and buckling-restrained braced frames. *Earthquake Engineering Structural Dynamic.* 50: 329–353.

Karavasilis T.L., Seo C.-Y. (2011). Seismic structural and non-structural performance evaluation of highly damped self-centering and conventional systems. *Engineering Structures*. 33(8):1859-1869.

Latour M., Rizzano G., Santiago A., Simoes da Silva L. (2019). Experimental response of a low-yielding, self-centering, rocking column base joint with friction dampers. *Soil Dynamics and Earthquake Engineering*. 116: 580–592.

Lettieri A., De la Peña A., Freddi F., Latour M. (2023). Damage-free self-centring links for eccentrically braced frames: development and numerical study. *Journal of Constructional Steel Research*. 201:107727

McKenna F., Scott M. H., Fenves, G. L. (2010). Non-linear Finite-Element Analysis Software Architecture Using Object Composition. *Journal of Computing in Civil Engineering*, 24(1):915 95–107.

Miranda E. Inelastic displacement ratios for structures on firm sites. (2000). *ASCE Journal of Structural Engineering*. 126(10):1150-1159.

Pei S., van de Lindt J. W., Barbosa A. R., Berman J. W., McDonnell E., Dolan J. D., Blomgren H.E., Zimmerman R. B., Huang D., Wichman S. (2019). Experimental Seismic Response of a Resilient 2-Story Mass-Timber Building with Post-Tensioned Rocking Walls. *ASCE Journal of Structural Engineering*. 145(11):04019120.

Pieroni L., Benedetto D. S., Freddi F., Latour M. (2022). Genetic algorithm for the optimal placement of self-centering damage-free joints in steel MRFs. *Journal of Constructional Steel Research*. 197:107489.

Pieroni L., Freddi F., Latour M. (2022) Effective placement of self-centering damage-free connections for seismic-resilient steel moment resisting frames. *Earthquake Engineering Structural Dynamic.* 51:1292–1316.

Priestley M.J.N., Calvi G.M., Kowalsky M.J. (2007). Displacement-Based Seismic Design of Structures. Pavia: IUSS Press.

Seo C.Y., Sause R. (2005) Ductility demands on self-centering systems under earthquake loading. *ACI Structural Journal*. 102(2):275

Shen Y., Freddi F., Li Y. (2022) Parametric experimental investigation of unbonded post-tensioned reinforced concrete bridge piers under cyclic loading. *Earthquake Engineering Structural Dynamic.* 51:3479–3504.

Tubaldi E., Ragni L., Dall' Asta A. (2014). Probabilistic seismic response assessment of linear systems equipped with nonlinear viscous dampers. 44:101–120

Veletsos A.S., Newmark N.M.. (1960). Effect of inelastic behavior on the response of simple systems to earthquake motions. *In: Proceedings of the 2nd World Conference on Earthquake Engineering,* Vol. 2; Japan: 89591.

Wang B., Nishiyama M., Zhu S., Tani M., Jiang H. (2021). Development of novel self-centering steel coupling beams without beam elongation for earthquake resilience. *Engineering Structures*. 232: 111827.

Zhong C., Christopoulos C. (2022). Self-centering seismic-resistant structures: Historical overview and state-of-the-art. *Earthquake Spectra*. 38(2):1321-1356.